FULL PAPER

Dalton
www.rsc.org/dalton

Synthesis and studies of a trinuclear Mn(II) carboxylate complex

Paul Christian,[a] Gopalan Rajaraman,[a] Andrew Harrison,[b] Madeleine Helliwell,[a] Joseph J. W. McDouall,[a] James Raftery[a] and Richard E. P. Winpenny*[b]

[a] *Department of Chemistry, The University of Manchester, Oxford Road, Manchester, UK M13 9PL*

[b] *Department of Chemistry, The University of Edinburgh, West Mains Road, Edinburgh, UK EH9 3JJ*

Received 11th May 2004, Accepted 17th June 2004
First published as an Advance Article on the web 19th July 2004

We report a carboxylate triangle consisting of three manganese(II) centres which is made from manganese(II) carbonate and pivalic acid. The magnetic exchange within the triangle is extremely weak, and antiferromagnetic. Several models have been used to fit the magnetic data, and the best fit uses two weak antiferromagnetic coupling constants of $J_1 = -0.588$ cm^{-1} and $J_2 = -0.855$ cm^{-1}. Exchange interactions between the metal centres has been calculated using DFT adopting all the three possible Heisenberg models for a trinuclear system and the results are compared with experimental values. Spin density distribution is used to analyse the nature of the coupling between the metal centres. EPR spectroscopy has been used to explore the nature of the ground state. Recrystallisation of the trinuclear compound from MeCN gives a polymer, while oxidation in air leads to a known compound—an edge-sharing bitetrahedral $\{Mn^{III}_2Mn^{II}_4\}$ cage.

Introduction

There are many examples in the literature of oxo-centred first row transition metal triangles where the metals are in the +3 oxidation state.[1] There are also examples of compounds where two metal centres are in the +3 oxidation state and the third is in the +2 state.[1,2] Examples where three paramagnetic M^{2+} form a triangle are more rare but are known for iron,[3] nickel,[4] cobalt[5] and copper.[6] There is only one example of a Mn(II) trimer bridged by carboxylates[7]—in general manganese carboxylate chemistry leads to higher oxidation states.[8] We were interested in making Mn(II) pivalate complexes as starting materials for the synthesis of clusters, in a manner analogous to the cobalt–pivalate chemistry we have been able to develop from a dinuclear cobalt(II) pivalate complex.[9] Here we report the synthesis of a triangular Mn(II) pivalate cage and a detailed study of its magnetic behaviour.

Experimental

Preparation of compounds

Manganese nitrate and potassium carbonate were obtained from Aldrich and used as received. Acetone, acetonitrile, trimethylacetic acid and deionised water were degassed before use.

Synthesis. *$[Mn_3(Me_3CCO_2)_6(Me_3CCO_2H)_5]\cdot 2(Me_3CCO_2H)$* ***1***. All operations were carried out under N_2; the presence of air at any stage leads to rapid oxidation to Mn(III) complexes. Manganese nitrate hexahydrate (16.3 g, 14.9 mmol) was dissolved in water (50 ml) and treated with a solution of potassium carbonate (12.0 g, 85.6 mmol) in water (50 ml). A pale precipitate formed immediately and the suspension was stirred for 0.5 h. The precipitate was separated by filtration and washed with water (2 × 100 ml) then acetone (100 ml). The powder was dried under vacuum to give $MnCO_3$ as a pale cream/white solid. Trimethylacetic acid (50.0 ml, 437 mmol) was slowly added to the solid with stirring, and the resulting suspension stirred for 24 h. (Note: heating the suspension resulted in oxidation of the manganese and formation of a Mn_6O_2 cage **3**). The reaction suspension was diluted with acetone (100 ml) and filtered through a 5 × 15 cm bed of Celite under N_2. Evaporation of the acetone under a flow of N_2 gave **1** as a crude product, yield 59.6%. Crystals of **1** were obtained by recrystallisation from a 1 : 1 acetone/acetonitrile solution at 4 °C. Elemental analysis: $Mn_3C_{60}H_{114}O_{24}$ expected: C 52.06, H 8.24; Found C 52.44, H 8.51.FT-IR, Nujol mull; (cm^{-1}), 1702(s), 1676(s), 1604(s), 1570(s), 1224(s), 1206(s), 1032, 938(b), 897, 874, 799, 789.

Table 1 Experimental data for the X-ray studies of **1** and **2**

Compound	**1**	**2**
Formula	$Mn_3C_{60}H_{114}O_{24}$	$Mn_4C_{50}H_{92}O_{20}$
M	1384.33	1233
Crystal system	Monoclinic	Triclinic
Space group	Pn	P-1
a/Å	12.2816(13)	11.682(5)
b/Å	31.569(4)	12.429(5)
c/Å	19.789(2)	21.966(5)
α/°	90	92.811(5)
β/°	90	95.884(5)
γ/°	90	98.736(5)
U/Å^3	7672.5(14)	3129(2)
T/K	100(2)	100(2)
Z	4	2
D_c/g cm^{-3}	1.198	1.309
μ/mm^{-1}	0.553	0.854
Unique data	44360	12641
Unique data with $F_o > 4\sigma F_o$	21193	11009
Parameters/restraints	1569/818	756/36
$R1$, $wR2$[a]	0.0452, 0.1129	0.0291, 0.0777

[a] $R1$ based on observed data, $wR2$ on all unique data.

$[Mn_4(Me_3CCO_2)_8(Me_3CCO_2H)_2]_n$ ***2***. **1** was dissolved in acetone/acetonitrile and the solution was allowed to evaporate at room temperature. After several days a few small crystals of **2** formed. The material was insoluble. Insufficient material was obtained for an elemental analysis.

$[Mn_6O_2(Me_3CCO_2)_{10}(THF)_4].THF$ ***3***. **1** (458 mg, 0.33 mmol) was dissolved in THF (5 ml) in air and allowed to stand for five days. The solution gradually darkened and large dark crystals of **3** formed. The identity of **3** was confirmed by a unit cell comparison with the previous report of this compound.[10] Yield 68%. Elemental analysis: expected C 47.71, H 7.40, Mn 19.84; found C 47.81, H 7.36, Mn 20.08. FT-IR (Nujol mull cm^{-1}) 1698, 1592(s), 1570(s) 1412(s), 1310, 1262, 1227, 1206, 1095(b), 1031, 937(w), 895, 872, 798, 787.

Crystallography

Crystal data and data collection and refinement parameters for compounds **1** and **2** are given in Table 1, selected bond lengths and angles in Tables 2–4.

DOI: 10.1039/b407126c

Table 2 Selected bond lengths [Å] and angles [°] for **1**

	Mol A	Mol B		Mol A	Mol B
Mn(1)–O(1)	2.066(4)	2.059(4)	Mn(2)–O(4)	2.214(4)	2.208(4)
Mn(1)–O(7)	2.157(4)	2.137(4)	Mn(2)–O(17)	2.222(4)	2.206(4)
Mn(1)–O(9)	2.198(4)	2.226(4)	Mn(2)–O(15)	2.291(4)	2.312(4)
Mn(1)–O(3)	2.202(4)	2.159(4)	Mn(3)–O(14)	2.114(4)	2.103(4)
Mn(1)–O(5)	2.202(4)	2.196(4)	Mn(3)–O(19)	2.129(4)	2.134(4)
Mn(1)–O(11)	2.273(4)	2.276(5)	Mn(3)–O(21)	2.134(4)	2.141(4)
Mn(2)–O(2)	2.067(4)	2.073(4)	Mn(3)–O(8)	2.144(4)	2.110(4)
Mn(2)–O(13)	2.111(4)	2.119(4)	Mn(3)–O(4)	2.326(4)	2.323(3)
Mn(2)–O(6)	2.179(4)	2.174(4)	Mn(3)–O(5)	2.354(4)	2.334(4)
O(1)–Mn(1)–O(7)	171.60(16)	170.14(17)	O(6)–Mn(2)–O(17)	162.62(15)	161.83(16)
O(1)–Mn(1)–O(9)	88.40(15)	86.10(16)	O(4)–Mn(2)–O(17)	96.84(14)	96.88(14)
O(7)–Mn(1)–O(9)	84.10(14)	84.91(15)	O(2)–Mn(2)–O(15)	93.28(16)	91.29(17)
O(1)–Mn(1)–O(3)	93.85(16)	94.74(16)	O(13)–Mn(2)–O(15)	83.13(16)	83.74(15)
O(7)–Mn(1)–O(3)	92.03(15)	92.63(16)	O(6)–Mn(2)–O(15)	82.48(16)	80.85(15)
O(9)–Mn(1)–O(3)	160.99(15)	162.58(16)	O(4)–Mn(2)–O(15)	172.97(16)	172.69(15)
O(1)–Mn(1)–O(5)	94.23(15)	94.17(16)	O(17)–Mn(2)–O(15)	80.14(15)	80.97(15)
O(7)–Mn(1)–O(5)	90.45(15)	90.71(15)	O(14)–Mn(3)–O(19)	88.19(17)	90.84(17)
O(9)–Mn(1)–O(5)	97.00(14)	95.31(15)	O(14)–Mn(3)–O(21)	91.31(17)	92.67(18)
O(3)–Mn(1)–O(5)	101.65(14)	101.97(15)	O(19)–Mn(3)–O(21)	103.90(13)	102.89(14)
O(1)–Mn(1)–O(11)	92.22(15)	90.84(17)	O(14)–Mn(3)–O(8)	179.01(19)	178.81(15)
O(7)–Mn(1)–O(11)	82.72(15)	83.68(16)	O(19)–Mn(3)–O(8)	92.72(17)	89.26(17)
O(9)–Mn(1)–O(11)	79.59(15)	80.49(16)	O(21)–Mn(3)–O(8)	88.10(17)	88.47(18)
O(3)–Mn(1)–O(11)	81.46(15)	82.11(16)	O(14)–Mn(3)–O(4)	89.54(14)	89.49(14)
O(5)–Mn(1)–O(11)	172.63(15)	173.25(15)	O(19)–Mn(3)–O(4)	166.10(15)	167.72(14)
O(2)–Mn(2)–O(13)	170.63(16)	170.53(17)	O(21)–Mn(3)–O(4)	89.86(14)	89.35(14)
O(2)–Mn(2)–O(6)	95.20(16)	94.75(17)	O(8)–Mn(3)–O(4)	89.67(14)	90.16(15)
O(13)–Mn(2)–O(6)	92.91(16)	92.42(16)	O(14)–Mn(3)–O(5)	90.23(14)	89.89(15)
O(2)–Mn(2)–O(4)	92.83(15)	95.54(16)	O(19)–Mn(3)–O(5)	88.04(15)	89.02(14)
O(13)–Mn(2)–O(4)	90.30(15)	89.13(14)	O(21)–Mn(3)–O(5)	168.00(15)	167.76(14)
O(6)–Mn(2)–O(4)	100.44(15)	101.12(14)	O(8)–Mn(3)–O(5)	90.19(14)	88.92(15)
O(2)–Mn(2)–O(17)	85.78(15)	85.88(16)	O(4)–Mn(3)–O(5)	78.25(10)	78.70(11)
O(13)–Mn(2)–O(17)	85.08(15)	85.38(15)			

Data collection and processing. Data were collected with a Bruker Smart APEX CCD area detector equipped with an Oxford Cryosystems low-temperature device,[11] using Mo–Kα radiation and ω scans. Data were corrected for Lorentz and polarisation factors. Absorption corrections were applied to all data.

Structure analysis and refinement. All structures were solved by direct methods using SHELXS-97. All structures were completed by iterative cycles of ΔF-syntheses and full-matrix least-squares refinement. All non-H atoms were refined anisotropically, except two disordered O atoms belonging to a pivalate ligand in **2**. In all structures difference Fourier syntheses were employed in positioning idealised methyl-hydrogen atoms which were assigned isotropic thermal parameters [U(H) = 1.5 U_{eq}(C)], and allowed to ride on their parent C-atoms [C–H 0.93 Å]. All refinements were against F^2 and used SHELXL-97.[12]

Additional material available from the Cambridge Crystallographic Data Centre comprises atom coordinates, thermal parameters and remaining bond lengths and angles.

CCDC reference numbers 238346 and 238347.

See http://www.rsc.org/suppdata/dt/b4/b407126c/ for crystallographic data in CIF or other electronic format.

Magnetic measurements

Variable temperature magnetic measurements in the region 1.8–350 K were made using a SQUID magnetometer (Quantum Design) with samples sealed in gelatin capsules. Diamagnetic corrections for sample holders and samples were applied to the data.

Results and discussion

Structures

1 crystallises in the space group *Pn*, with two independent molecules of the cluster in the asymmetric unit. Both molecules have the same structure (Fig. 1) consisting of a triangle of six-coordinate Mn(II) ions face-capped by two 3.21-bridging pivalates (Harris notation[13]). The edges of the triangle are bridged by three further 2.11 pivalates. The remaining positions on each Mn site are, in each case, occupied by two molecules of pivalic acid or pivalate; for Mn(1) and Mn(2) these are both neutral molecules, which form H-bonds to 2.11 bridging pivalates [*e.g.* O(10)···H···O(7)]. The O···O distances for these H-bonds vary from 2.56 to 2.63 Å. For Mn(3) there is a short H-bond between the two terminal molecules [O(20)···O(22) 2.409(6) Å], suggesting one is a pivalate and the second a pivalic acid. Two molecules of pivalic acid are also found in the unit cell. Selected bond lengths and angles are given in Table 2.

The structure therefore introduces the possibility of two distinct super-exchange paths for magnetic interactions. While each edge has a 2.11 bridging pivalate, the Mn(1)···Mn(3) and Mn(2)···Mn(3) contacts are further bridged by a μ_2-O atom from the 3.21 pivalate [O(5) and O(4) respectively]. The Mn(1)···Mn(2) contact does

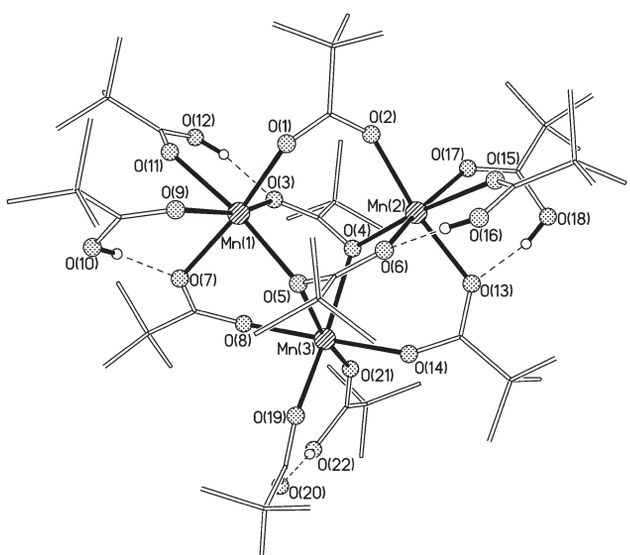

Fig. 1 The structure of **1** in the crystal. C-atoms shown as lines and H-atoms omitted for clarity. H-bonds shown as dashed lines.

Table 3 Selected bond lengths (Å) and angles (°) for **2**

Mn(1)–O(2)	2.1030(12)	Mn(3)–O(12)	2.0825(13)
Mn(1)–O(16)	2.1043(14)	Mn(3)–O(13)	2.1896(14)
Mn(1)–O(9)	2.1587(12)	Mn(3)–O(7)	2.1905(12)
Mn(1)–O(14)	2.1992(13)	Mn(3)–O(10)	2.2113(14)
Mn(1)–O(17)	2.2079(13)	Mn(3)–O(6)	2.2115(14)
Mn(1)–O(4)	2.3918(13)	Mn(3)–O(20)	2.2228(12)
Mn(2)–O(18)	2.0808(13)	Mn(4)–O(15)	2.0828(13)
Mn(2)–O(1)	2.0967(13)	Mn(4)–O(19)	2.1420(13)
Mn(2)–O(11)	2.1335(12)	Mn(4)–O(5)	2.1514(13)
Mn(2)–O(20)	2.1974(14)	Mn(4)–O(4)	2.2205(12)
Mn(2)–O(10)	2.2850(12)	Mn(4)–O(13)	2.2571(12)
Mn(2)–O(9)	2.3510(13)	Mn(4)–O(14)	2.3769(13)
O(2)–Mn(1)–O(16)	90.65(5)	O(12)–Mn(3)–O(13)	99.62(4)
O(2)–Mn(1)–O(9)	100.40(5)	O(12)–Mn(3)–O(7)	89.56(5)
O(16)–Mn(1)–O(9)	93.18(5)	O(13)–Mn(3)–O(7)	88.84(4)
O(2)–Mn(1)–O(14)	159.40(5)	O(12)–Mn(3)–O(10)	91.67(4)
O(16)–Mn(1)–O(14)	92.76(5)	O(13)–Mn(3)–O(10)	167.58(4)
O(9)–Mn(1)–O(14)	99.68(5)	O(7)–Mn(3)–O(10)	96.47(4)
O(2)–Mn(1)–O(17)	85.71(5)	O(12)–Mn(3)–O(6)	173.09(4)
O(16)–Mn(1)–O(17)	165.62(5)	O(13)–Mn(3)–O(6)	84.15(4)
O(9)–Mn(1)–O(17)	101.15(4)	O(7)–Mn(3)–O(6)	84.70(5)
O(14)–Mn(1)–O(17)	85.98(5)	O(10)–Mn(3)–O(6)	85.16(4)
O(2)–Mn(1)–O(4)	83.44(5)	O(12)–Mn(3)–O(20)	88.72(5)
O(16)–Mn(1)–O(4)	84.33(4)	O(13)–Mn(3)–O(20)	92.13(4)
O(9)–Mn(1)–O(4)	175.47(4)	O(7)–Mn(3)–O(20)	178.15(4)
O(14)–Mn(1)–O(4)	76.70(5)	O(10)–Mn(3)–O(20)	82.90(4)
O(17)–Mn(1)–O(4)	81.44(4)	O(6)–Mn(3)–O(20)	96.96(5)
O(18)–Mn(2)–O(1)	92.75(6)	O(15)–Mn(4)–O(19)	175.07(5)
O(18)–Mn(2)–O(11)	86.84(5)	O(15)–Mn(4)–O(5)	87.00(5)
O(1)–Mn(2)–O(11)	175.47(5)	O(19)–Mn(4)–O(5)	91.83(5)
O(18)–Mn(2)–O(20)	126.60(5)	O(15)–Mn(4)–O(4)	90.63(5)
O(1)–Mn(2)–O(20)	87.85(4)	O(19)–Mn(4)–O(4)	85.09(4)
O(11)–Mn(2)–O(20)	88.78(4)	O(5)–Mn(4)–O(4)	106.03(5)
O(18)–Mn(2)–O(10)	149.76(5)	O(15)–Mn(4)–O(13)	102.00(5)
O(1)–Mn(2)–O(10)	99.21(5)	O(19)–Mn(4)–O(13)	82.69(5)
O(11)–Mn(2)–O(10)	83.29(5)	O(5)–Mn(4)–O(13)	121.60(5)
O(20)–Mn(2)–O(10)	81.79(4)	O(4)–Mn(4)–O(13)	130.98(4)
O(18)–Mn(2)–O(9)	94.87(5)	O(15)–Mn(4)–O(14)	91.43(5)
O(1)–Mn(2)–O(9)	96.92(5)	O(19)–Mn(4)–O(14)	89.96(5)
O(11)–Mn(2)–O(9)	87.60(5)	O(5)–Mn(4)–O(14)	176.92(4)
O(20)–Mn(2)–O(9)	138.08(4)	O(4)–Mn(4)–O(14)	76.62(5)
O(10)–Mn(2)–O(9)	56.31(4)	O(13)–Mn(4)–O(14)	56.16(4)

Table 4 B3LYP/TZV spin densities on atoms for configurations SC_1–SC_3

Atom[a]	SC_1	SC_2	SC_3	SC_4
Mn1	4.834	4.832	4.832	−4.831
Mn2	4.834	−4.831	4.832	4.833
Mn3	4.837	4.835	−4.835	4.836
O4	0.026	0.012	0.026	−0.012
O5	0.025	−0.011	0.025	0.011
O6	0.024	0.008	0.014	0.001
O7	0.004	−0.002	0.005	0.001
O8	0.006	0.002	0.008	−0.004
O9	0.025	−0.001	0.017	0.010
O10	0.020	0.020	0.010	−0.011
O11	0.015	0.015	−0.007	0.007
O12	0.021	−0.010	0.010	−0.007
O13	0.016	0.006	−0.006	−0.002
C1	0.025	0.001	0.024	0.000
C2	0.037	0.003	0.010	0.024
C3	0.035	0.020	0.012	0.002
C4	0.019	0.019	−0.002	0.002
C5	0.023	0.004	−0.004	0.023

[a] See Fig. 4 for atom numbering.

not have such a path, with and super-exchange passing through the O–C–O of the two 3.21 pivalates. In principle therefore the magnetic behaviour should be modelled as an isosceles triangle, rather than as an equilateral triangle. Whether this is necessary is discussed below.

2 crystallises with a 1D-polymeric structure, based on a $\{Mn_4\}$ repeat unit (Fig. 2). All Mn(II) sites are six-coordinate, with irregular geometries. The Mn···Mn vectors in the chain are bridged in four distinct ways. Mn(1)···Mn(2) is bridged by two 2.11 pivalates and a

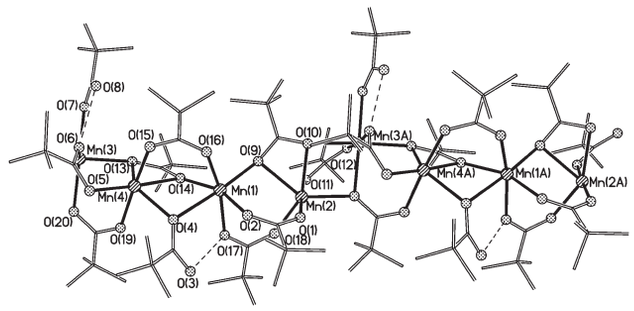

Fig. 2 The structure of **2** in the crystal. C-atoms shown as lines and H-atoms omitted for clarity. H-bonds shown as dashed lines.

μ_2-O atom [O(9)] from a 3.22 pivalate. Mn(1)···Mn(4) is bridged by a single 2.11 carboxylate, a μ_2-O atom [O(14)] from a 3.22 pivalate and a μ_2-O atom [O(4)] from a 2.20 pivalic acid. Mn(3)···Mn(4) is bridged by a 2.11 carboxylate, a 3.21 carboxylate and a μ_2-O atom [O(13)] from a 3.22 pivalate. Finally Mn(2)···Mn(3a) is bridged by a 2.11 pivalate [O(11) and O(12)] and two μ_2-O atoms from a 3.21 pivalate and a 3.22 pivalate [O(10)].

The structure demonstrates the coordinative flexibility that pivalate can show. Of the eight pivalates, two show a 3.22 binding mode, which has previously been found for acetate[14] and benzoate.[15] One shows the 3.21 mode (also seen in **1**) and five show the typical 2.11 mode found for most carboxylates. The structure also contains a 2.20 pivalic acid, and a terminal pivalic acid attached to Mn(3). The protonated O-atoms of the pivalic acids form H-bonds to bridging pivalates with O···O distances of 2.61 Å. Selected bond lengths and angles are given in Table 3.

If air is allowed into the reaction that gives **1**, or if **1** is deliberately oxidised a mixed-valent hexanuclear cage $[Mn_6O_2(Me_3CCO_2)_{10}(THF)_4]$ **3** is formed, which we have previously reported.[10] The core of the structure is an edge-sharing bitetrahedron, with each tetrahedron centred about a μ_4-oxide. The two Mn(III) ions are in the shared-edge, while the four Mn(II) centres lie at the periphery of the molecule.

Magnetic properties

The magnetic susceptibility of **1** was measured between 2 and 320 K (Fig. 3). Analysis of the data shows that the room temperature value of $\chi_m T$ (where χ_m is the molar magnetic susceptibility) of 13.0 cm^3 K mol^{-1}, is very close to that calculated for three non-interacting $S = 5/2$ centres and $g = 1.99$. $\chi_m T$ is constant as the temperature is lowered to 70 K, after which it begins to fall gradually. At the lowest temperature measured $\chi_m T$ has a value of 1.3 cm^3 K mol^{-1}. This behaviour suggests weak antiferromagnetic exchange between the Mn(II) centres, leading to a non-zero ground state.

The structure consists of an isosceles triangle, which suggests the most accurate spin Hamiltonian should contain two exchange interactions (eqn [1]):

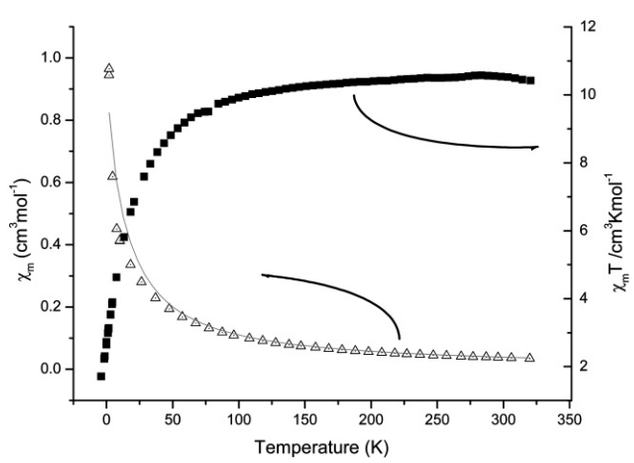

Fig. 3 Plot of χ_m and $\chi_m T$ *vs.* T for **1**. Triangles: measured χ_m; squares, measured χ_mT; solid line: fit as described in text.

$$H = -2J_1(S_1S_2 + S_2S_3) - 2J_2S_1S_3 \quad (1)$$

The best fit of the variable temperature behaviour of χ_m is for $J_1 = -0.59$ and $J_2 = -0.86$ cm^{-1}. The fit is shown in Fig. 3. The quality of the fit gives $R^2 = 0.9994$. However, given the very small and similar values of J_1 and J_2 it seemed sensible to perform the calculation where J_1 and J_2 are constrained to be equal, *i.e.* to treat the problem as an equilateral triangle. This gave a single exchange interaction of −0.51 cm^{-1}, but with slightly less good statistics: $R^2 = 0.9455$. The two *J*-model therefore fits the data better, but it is very doubtful whether the statistical improvement obtained justifies the introduction of this additional parameter. As the two exchange paths are distinct it is perhaps surprising that the fit is so insensitive to the model used. The implication is that little magnetic information is conveyed through the μ_2-O atoms from the 3.21 pivalate ligands in this case.

The experimental *J* values have been used to generate the Eigenfunction of the spin states involved using MAGPACK software.[16] The ground spin state was found to be $S = 1/2$, with other excited states (such as $S = 3/2$ and $S = 5/2$) differing from the ground state by only a few wavenumbers. The very small exchange coupling found here increases the uncertainty in assigning a unique spin ground state to **1**, however, such uncertainty is quite common in triangular species where competing antiferromagnetic exchange interactions are present.

Computational studies

Recently there has been a great deal of interest in the evaluation of magnetic exchange couplings using the techniques of quantum chemistry.[17,18] For larger systems the most widely used scheme is Noodleman's (broken symmetry) valence bond description based on non-orthogonal magnetic orbitals, derived from a spin-unrestricted reference wavefunction.[19] Noodleman's approach coupled with widely used exchange–correlation functionals has been shown to yield exchange coupling constants with good accuracy at a modest computational cost. Accordingly, all calculations here have used the B3LYP functional[20] with the valence triple-zeta quality basis sets (TZV) of Ahlrichs and coworkers.[21] There is a good body of evidence in the literature[22] that the B3LYP/TZV level of theory yields accurate predictions of magnetic coupling constants. All calculations were performed using the GAUSSIAN 98 suite of programs,[23] with an initial guess made using Jaguar 5.0.

Most computational studies have concentrated on binuclear metallic complexes,[24] but recently polymetallic systems have been studied. Ruiz *et al.*[25] have advocated the approximation of polynuclear magnetic couplings as a sum of pairwise interactions. We have used this approach to calculate exchange interactions in several iron(III) and chromium(III) clusters.[26] To justify this approach, recall that when using density functional theory the magnetic coupling, J_1, in a binuclear system, with spins S_1 and S_2, can be expressed in terms of the difference between the energy of the broken symmetry state (equivalent to the low spin state) and that of the high spin state as:

$$J = \frac{(E_{BS} - E_{HS})}{2S_1S_2 + S_2} \quad (2)$$

1 may be depicted schematically as in Scheme 1. There are three possibilities:

Model A. The trinuclear unit has no symmetry which implies that there can be three independent couplings, to account for the exchange interaction between the metal centers. ($J_1 \neq J_2 \neq J_3$ in Scheme 1). The spin Hamiltonian is then:

$$\hat{H} = -2J_1\hat{S}_1\hat{S}_2 - 2J_2\hat{S}_2\hat{S}_3 - 2J_3\hat{S}_3\hat{S}_1 \quad (3)$$

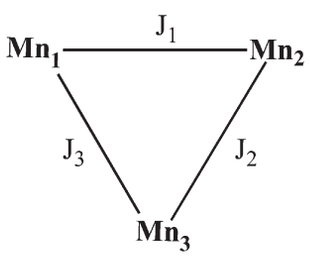

Scheme 1

Model B. As Mn_1 and Mn_2 are chemically equivalent we need only consider two coupling constants. ($J_1 \neq J_2 = J_3$ in Scheme 1). The relevant spin Hamiltonian is given in eqn. [1].

Model C. We could assume only the coupling between each metal centre is equivalent. ($J_1 = J_2 = J_3$ in Scheme 1). The spin Hamiltonian is then:

$$\hat{H} = -2J_1(\hat{S}_1\hat{S}_2 + \hat{S}_2\hat{S}_3 + \hat{S}_3\hat{S}_1) \quad (4)$$

The original crystal structure has been simplified for the calculations by replacing the pivalate groups with acetate (Fig. 4). Assuming that magnetically the system may be described as a sum of pairwise interactions as in eqn. [2], then the exchange interactions can be evaluated using the energy differences of the possible spin configurations (SC). The chosen spin configurations are shown in Scheme 2; as we wish to calculate three exchange terms for Model A, we need consider four spin configurations.

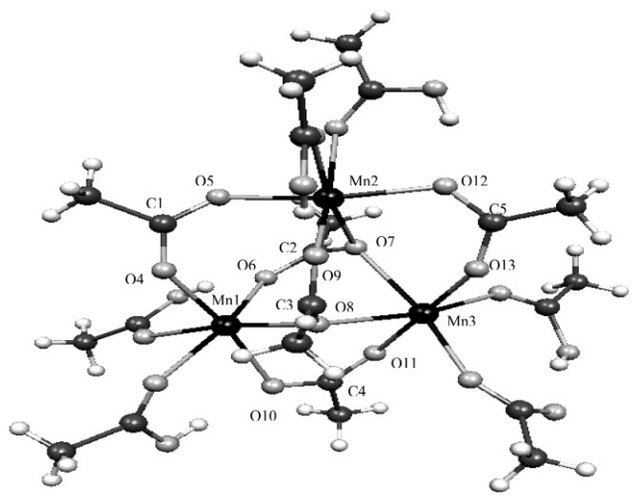

Fig. 4 The model structure and numbering scheme used for the DFT calculations on **1**.

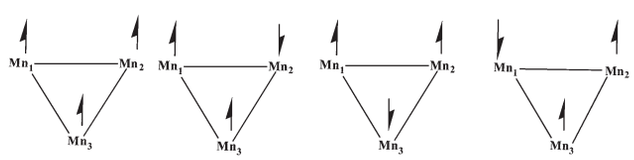

Scheme 2

B3LYP/TZV calculations on these configurations yielded the spin densities given in Table 4. The modulus of the spin densities on each Mn unit is >4.8 indicating that the magnetic orbitals are centred on the metals, with relatively little delocalization. The signs of the spin densities also confirm that we have successfully obtained the spin configurations of Scheme 2. The relative energies of SC_1–SC_4 are depicted in Fig. 5.

Applying eqn. [2] to each pairwise interaction between the Mn centres in SC_1–SC_4 to calculate three independent couplings J_1, J_2 and J_3 yields the following relationships from which J_1, J_2 and J_3 may be evaluated.

$$\frac{(E_{SC1} - E_{SC2})}{15} = -2J_1 - 2J_2 \quad (5)$$

$$\frac{(E_{SC1} - E_{SC3})}{15} = -2J_2 - 2J_3 \quad (6)$$

$$\frac{(E_{SC1} - E_{SC4})}{15} = -2J_1 - 2J_3 \quad (7)$$

Table 5 Calculated exchange interactions (cm^{-1}) for the three models

Exchange interaction	Model A	Model B	Model C
J_1	−1.81	−1.80	−1.68
J_2	−1.69	−1.62	N/A
J_3	−1.56	N/A	N/A

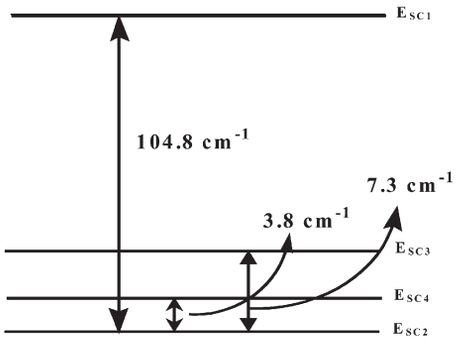

Fig. 5 The relative energies of the four spin configurations calculated for **1**.

All calculated couplings are antiferromagnetic (Table 5), and the magnitude of the couplings are almost the same. To calculate the two coupling constants for model B, eqns. [5]–[7] can be simplified by considering, $J_2 = J_3$. J_1 can be calculated using either eqn. [5] or [7], the calculation yields almost the same value and the average value is shown in Table 5. For model C, energies are only required for two spin configurations, and this can be calculated using eqn. [5], [6] or [7]. The value shown in Table 5 is the average of three values obtained. Regardless of the model, the calculated couplings are antiferromagnetic and all of them are almost of the same magnitude. The experimental fitting gives $J_1 = -0.59$ cm^{-1} and $J_2 = -0.86$ cm^{-1} and the agreement between DFT and fitting is very good. A similar Mn(II) system reported in the literature also has a very small coupling constant.[27]

The spin density distribution suggests that the main mechanism for exchange is spin delocalisation.[28] From Table 4, the spin density on the bridging oxygen atoms is approximately 0.02 (*e.g.*, O_4, O_5, O_6 *etc.*) except for O_7 and O_8 the spin densities are smaller (0.003 and 0.006, respectively); these oxygen atoms are the two μ_2-O atoms of the 3.21 bridging pivalates. The reverse trend may be seen on the carbon atoms. This implies very little magnetic information is passed through these μ_2-O atoms and that the predominant exchange path is through the 2.11 bridging pivalates. This, in turn, justifies the very similar exchange interactions for all paths in **1**; the geometric differences do not cause differences in the exchange paths.

EPR spectroscopy

The variable temperature EPR spectra of a powder sample of **1** was measured at Q-band (Fig. 6). An isotropic signal appears at $g = 2.00$ at room temperature, due to population of all states in the system. At 5 K there are also weak resonances at around $g = 4$, in addition to strong resonances around $g = 2$. In principle, the temperature dependence of these two signals could be used as a guide to predict the ground state of the molecule. If the intensity of the features at $g = 4$ increases with decreasing temperature, this would indicate a spin ground state with $S > 1/2$, and some zero-field splitting of that state. If a signal at $g = 2.00$ gained intensity with decreasing temperature this would support an $S = 1/2$ ground state. The EPR spectrum at 5 K has been simulated using the SIMEPR simulation code with the spin Hamiltonian parameters; $S = 3/2$, $D = 0.050$ cm^{-1}, $E = 0.008$ and $g = 1.97$, with the line width of $W_x = 200$, $W_y = 200$, $W_z = 350$ Gauss. The simulated and experimental spectrum is shown in Fig. 6. The simulated spectrum does not reproduce all the signals; this suggests that there are contributions from other spin states even at this temperature. Therefore, as suggested by the *J*-values derived above, the ground state and low-lying excited states of **1** are very close in energy and several such states are populated even at 5 K.

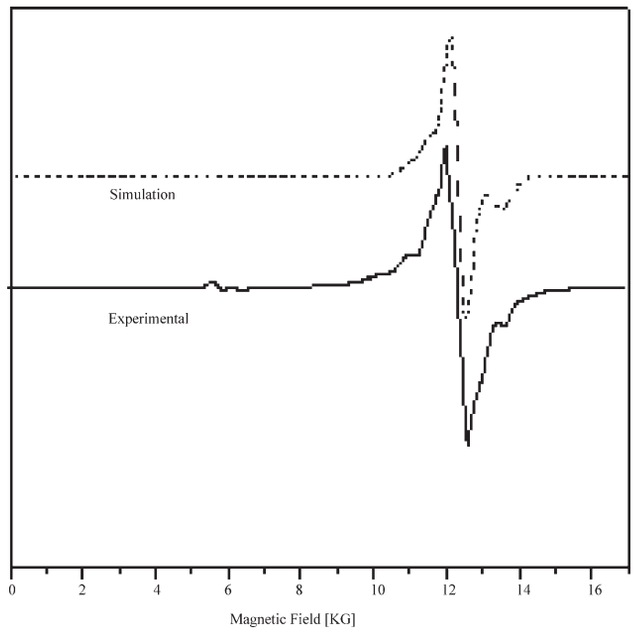

Fig. 6 Observed and simulated Q-band EPR spectrum of a powdered sample of **1**; the observed spectrum was measured at 5 K.

Conclusion

1 is a rare example of a non-oxo centred metal triangle and therefore we have spent some effort understanding its magnetic behaviour. The conclusion is that the exchange paths in the molecule are extremely weak, and that despite the difference in the nature of the chemical bridge between the Mn(II) ions in the various paths no significant difference between the magnitude of the exchange in these two paths can be discerned. DFT calculations support this conclusion, finding little spin density on the μ_2-O atoms of the 3.21 bridging pivalates which would be required if this path were to be distinct.

Acknowledgements

We thank the EPSRC for funding for the SQUID susceptometer and the University of Manchester for support. We would like to thank the EPSRC UKCCF for computer time on the Columbus system and also the University of Manchester Computing Centre for access to the Bezier high performance computing facility.

References

1 R. D. Cannon and R. P. White, *Prog. Inorg. Chem*, 1988, **36**, 195.
2 S. P. Palii, D. E. Richardson, M. L. Hansen, B. B. Iversen, F. K. Larsen, L. Singerean, G. A. Timco, N. V. Gerbeleu, K. R. Jennings and J. R. Eyler, *Inorg. Chim. Acta*, 2001, **319**, 23.
3 S. K. Mandal, V. G. Young, Jr. and L. Que, Jr., *Inorg. Chem.*, 2000, **39**, 1831; C. Boskovic, E. Rusanov, H. Stoeckli-Evans and H. U. Güdel, *Inorg. Chem. Commun.*, 2002, **5**, 881.
4 R. Kempe, J. Sieler, D. Walther, J. Reinhold and K. Rommel, *Z. Allorg. Allg. Chem.*, 1993, **619**, 1105.
5 J. Estienne and R. Weiss, *J. Chem. Soc., Chem. Commun.*, 1972, 862.
6 R. Clerac, F. A. Cotton, K. R. Dunbar, E. M. Hillard, M. A. Petrukhina and B. W. Smucker, *C. R. Acad. Sci. Ser. II Chim.*, 2001, **4**, 315.
7 K. Tsubeyoshi, H. Kobayashi and H. Miyamee, *Acta Crystallogr., Sect. C*, 1993, **49**, 233.
8 G. Aromi, S. M. J. Aubin, M. A. Bolcar, G. Christou, H. J. Eppley, K. Folting, D. N. Hendrickson, J. C. Huffman, R. C. Squire, H.-L. Tsai, S. Wang and M. W. Wemple, *Polyhedron*, 1998, **17**, 3005.
9 G. Aromi, A. S. Batsanov, P. Christian, M. Helliwell, A. Parkin, S. Parsons, A. A. Smith, G. A. Timco and R. E. P. Winpenny, *Chem. Eur. J.*, 2003, **9**, 5142.
10 M. Murrie, S. Parsons and R. E. P. Winpenny, *J. Chem. Soc., Dalton Trans.*, 1998, 1423.
11 J. Cosier and A. M. Glazer, *J. Appl. Crystallogr.*, 1986, **19**, 105.
12 *SHELXL-PC Package*. Bruker Analytical X-ray Systems: Madison, WI, 1998.
13 R. A. Coxall, S. G. Harris, D. K. Henderson, S. Parsons, P. A. Tasker and R. E. P. Winpenny, *J. Chem. Soc., Dalton Trans.*, 2002, 2349.

14 A. J. Taspiopaulos, N. C. Harden, K. A. Abboud and G. Christou, *Polyhedron*, 2003, **22**, 133.
15 C. Chen, J. Chen, H. Zhu, Z. Haung and Q. Liu, *Sci. China, Ser. B*, 2001, **44**, 320.
16 J. J. B. Almenar, J. M. C. Juan, E. Coronado and B. D. Tsukerblat, *Inorg. Chem.*, 1999, **38**, 6081.
17 N. Suaud, H. Bolvin and J. Daudey, *Inorg. Chem.*, 1999, **38**, 6089.
18 C. Graaf, C. Sousa, I. P. R. Moreira and F. Illas, *J. Phys. Chem. A*, 2001, **105**, 11371.
19 L. Noodleman, *J. Chem. Phys.*, 1981, **74**, 5737.
20 A. D. Becke, *J. Chem. Phys.*, 1993, **98**, 5648.
21 (*a*) A. Schäfer, H. Horn and R. Ahlrichs, *J. Chem. Phys.*, 1992, **97**, 2571; (*b*) A. Schäfer, C. Huber and R. Ahlrichs, *J. Chem. Phys.*, 1994, **100**, 5829.
22 E. Ruiz, S. Alvarez, J. Cano and P. Alemany, *J. Comput. Chem.*, 1999, **20**, 1391.
23 *Gaussian 98*, Revision A.11.3, M. J. Frisch, G. W. Trucks, H. B. Schlegel, G. E. Scuseria, M. A. Robb, J. R. Cheeseman, V. G. Zakrzewski, J. A. Montgomery, Jr., R. E. Stratmann, J. C. Burant, S. Dapprich, J. M. Millam, A. D. Daniels, K. N. Kudin, M. C. Strain, O. Farkas, J. Tomasi, V. Barone, M. Cossi, R. Cammi, B. Mennucci, C. Pomelli, C. Adamo, S. Clifford, J. Ochterski, G. A. Petersson, P. Y. Ayala, Q. Cui, K. Morokuma, N. Rega, P. Salvador, J. J. Dannenberg, D. K. Malick, A. D. Rabuck, K. Raghavachari, J. B. Foresman, J. Cioslowski, J. V. Ortiz, A. G. Baboul, B. B. Stefanov, G. Liu, A. Liashenko, P. Piskorz, I. Komaromi, R. Gomperts, R. L. Martin, D. J. Fox, T. Keith, M. A. Al-Laham, C. Y. Peng, A. Nanayakkara, M. Challacombe, P. M. W. Gill, B. Johnson, W. Chen, M. W. Wong, J. L. Andres, C. Gonzalez, M. Head-Gordon, E. S. Replogle, and J. A. Pople, Gaussian, Inc., Pittsburgh PA, 2002.
24 For example, C. J. Calzado, J. Cabrero, J. P. Malrieu and R. Caballol, *J. Chem. Phys.*, 2002, **116**, 2728 and references therein.
25 E. Ruiz, A. R. Fortea, J. Cano, S. Alvarez and P. Alemany, *J. Comput. Chem.*, 2003, **24**, 982; E. Ruiz, J. Cano, S. Alvarez, A. Caneschi and D. Gatteschi, *J. Am. Chem. Soc.*, 2003, **152**, 6791.
26 P. Christian, G. Rajaraman, A. Harrison, J. J. W. McDouall, J. T. Raftery and R. E. P. Winpenny, *Dalton Trans*, 2004, 1511; A.-A. H. Abu-Nawwas, J. Cano, P. Christian, T. Mallah, G. Rajaraman, S. J. Teat, R. E. P. Winpenny and Y. Yukawa, *Chem. Commun.*, 2004, 314; G. Rajaraman, J. Cano, E. K. Brechin and E. J. L. McInnes, *Chem. Commun.*, 2004, 1476.
27 D. Huang, X. Zhang, C. Chen, F. Chen, Q. Liu, D. Liao, L. Li and L. Sun, *Inorg. Chim. Acta*, 2003, **353**, 284.
28 J. Cano, E. Ruiz, S. Alvarez and M. Verdaguer, *Commun. Inorg. Chem.*, 1998, **20**, 27.